1-1-2007

Motion tracking control of piezo-driven flexure-based mechanism based on sliding mode strategy

Hwee Choo Liaw
Monash University

Bijan Shirinzadeh
Monash University

Julian Smith
Monash University

Gursel Alici
University of Wollongong, gursel@uow.edu.au

Motion Tracking Control of Piezo-Driven Flexure-Based Mechanism based on Sliding Mode Strategy

Hwee Choo Liaw, Bijan Shirinzadeh, Julian Smith, Gursel Alici

Abstract— **This paper presents a motion tracking control methodology based on sliding mode strategy for a flexure-based micro/nano manipulator driven by a piezoelectric actuator. This control methodology is proposed for tracking of desired motion trajectories in the presence of uncertain system parameters, non-linearities including the hysteresis effect, and external disturbances in the control system. In this paper, a four-bar link is investigated and a lumped parameter dynamic model is established for the formulation of the proposed sliding mode motion control methodology. The convergence of the position tracking error to zero is assured by the approach in the presence of the aforementioned conditions. The stability of the closed-loop system is proven theoretically, and a precise tracking performance in following a desired motion trajectory is demonstrated in the experimental study. With the capability of motion tracking, the proposed control methodology can be employed in realising high performance flexure-based control applications.**

I. Introduction

High-precision motion tasks in the field of micro/nano manipulation are generally accomplished by employing flexure-based mechanisms driven by piezoelectric actuators [1]. Generally, in the studies of the flexure-based mechanisms, the emphasis has been confined to the mechanical design, kinematic modelling, and stiffness analysis [2]–[5]. Little effort has been made to implement the motion tracking control for such mechanisms. Furthermore, there are other obstacles to the establishment of an effective control of the mechanisms. One of the prominent issues is the presence of non-linearity in the piezoelectric actuators driving the mechanisms. This nonlinear effect prevents the piezo-driven mechanisms from providing the desired high-precision motion resolution and accuracy.

A number of studies have therefore been conducted to resolve this nonlinear behaviour in the piezoelectric actuators. One focus of studies has been conducted to model and compensate for the non-linearities, particularly for the nonlinear hysteresis effect. Other areas of research have been focused on the enhancement of positioning performance by developing closed-loop control for the piezoelectric actuators.

H.C. Liaw and B. Shirinzadeh are with the Robotics and Mechatronics Research Laboratory, Department of Mechanical Engineering, Monash University, Clayton, VIC 3800, Australia (e-mail: hwee-choo.liaw @eng.monash.edu.au; bijan.shirinzadeh@eng.monash.edu.au).

J. Smith is with the Department of Surgery, Monash Medical Centre, Faculty of Medicine, Nursing and Health Sciences, Monash University, Clayton, VIC 3800, Australia (e-mail: julian.smith@med.monash.edu.au).

G. Alici is with the School of Mechanical, Materials, and Mechatronic Engineering, University of Wollongong, NSW 2522, Australia (e-mail: gursel@uow.edu.au).

Modelling techniques for the piezoelectric actuators have been studied. These include a voltage-input electromechanical model [6], a charge steering model [7], a model of physical hysteresis [8], a method for describing the nonlinear hysteresis [9], and a neural network hysteresis model [10]. However, the nonlinear hysteresis effect is very complex. It is difficult to obtain an accurate model and the model parameters are also difficult to quantify in practice.

Alternatively, appropriate closed-loop control strategies have been proposed to achieve the desired positioning accuracy for the piezoelectric actuators. Recent examples include a combination of a feed-forward model in a feedback control with an input shaper [11], an adaptive back-stepping approach [12], and a tracking control of a piezo-ceramic actuator with a feed-forward hysteresis compensation [13]. In most of these studies, a complex hysteresis model has been adopted to compensate for the nonlinear hysteresis effect, and furthermore, the research has been restricted to the piezoelectric actuators without involving the flexure-based mechanism.

In this paper, a motion tracking control methodology is established and investigated for a flexure-based mechanism, particularly for the flexure-hinged micro/nano manipulator. The proposed control methodology is based on sliding mode strategy and it is formulated without using any form of feed-forward compensation. This work is motivated by our previous efforts in the control of the piezoelectric actuators [14], [15]. The control objective is to track a specified motion trajectory in the proposed closed-loop system. In this research, a fundamentally important mechanism, a four-bar link, is employed as many of the complex manipulators can be constructed from the combination of such four-bar links [16].

The proposed control methodology is employed to accommodate uncertain system parameters, non-linearities including the hysteresis effect, and external disturbances in the flexure-based micro/nano manipulation system. In this study, a lumped parameter dynamic model is formulated for describing the piezo-driven flexure-based four-bar micro/nano manipulator. A sliding mode motion tracking control methodology is established based on the lumped parameter dynamic model. Stability analysis is performed in which the position tracking error is proved to be converging to zero in tracking of a desired motion trajectory. Furthermore, a precise motion tracking performance is demonstrated in the experimental study.

This paper is organised as follows. The model of a piezo-driven flexure-based four-bar micro/nano manipulator

1-4244-1264-1/07/$25.00 ©2007 IEEE

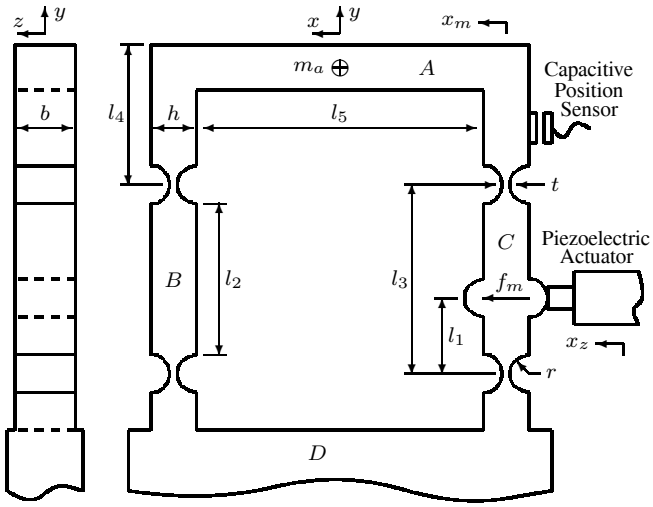

Fig. 1. Piezo-driven flexure-based four-bar micro/nano manipulator

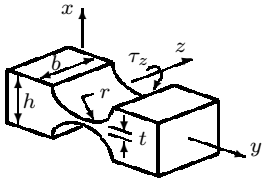

Fig. 2. Notch-type flexure hinge

is described in Section II. The proposed sliding mode motion tracking control methodology is established in Section III. The experimental study is detailed in Section IV and the results are presented and discussed in Section V. Finally, conclusions are drawn in Section VI.

II. Model of Piezo-Driven Flexure-Based Four-Bar Micro/Nano Manipulator

A piezo-driven flexure-based four-bar micro/nano manipulator under investigation is shown in Fig. 1. This manipulator is constructed by links and flexure hinges. It is assumed that the links are rigid and the flexure hinges are compliant in bending about one axis but rigid about the cross axes. The flexure hinge used is a notch-type hinge and the schematic of such hinge is shown in Fig. 2. Usually, the flexure hinge is simple in shape and operation; however, it is mathematically complex. For an angular deflection α_z about the z-axis due to an application of moment τ_z, the angular stiffness $k_{\tau_z\alpha_z}$ can be approximated by [17]

$$k_{\tau_z\alpha_z} \triangleq \frac{\tau_z}{\alpha_z} \approx \frac{2\,E\,b\,t^{\frac{5}{2}}}{9\,\pi\,r^{\frac{1}{2}}}\,, \tag{1}$$

where E is the elastic modulus of the flexure material, and b, r, t are the dimensions as shown in Fig. 1 and Fig. 2. It must be noted that the angular stiffness (1) is derived for the right circular flexure hinge, i.e. $h = 2\,r + t$.

As shown in Fig. 1, with the assumption of perfect hinge rotations and small displacements, an approximated rectilinear motion x_m is provided by the upper moving link A of the mechanism in the x-axis direction. Lagrangian analysis for a flexure-based mechanism [16] can be employed to formulate a dynamic model for describing the motion x_m. Using this analytical approach, the equation governing the motion of link A can be written as

$$\left(m_a + \frac{I_b + I_c}{{l_3}^2}\right)\ddot{x}_m + \frac{4\,k_{\tau_z\alpha_z}}{{l_3}^2}\,x_m = f_m\,, \tag{2}$$

where f_m is the applied force, m_a is the mass of link A, and I_b and I_c are the moments of inertia of links B and C, respectively, and l_3 is the parameter as shown in Fig. 1.

For the purpose of motion tracking control, a lumped parameter dynamic model that combines the flexure-based mechanism and the piezoelectric actuator can be formulated. This can be achieved by extending the model of a piezoelectric actuator [15], which is given by

$$m_z\,\ddot{x}_z + b_z\,\dot{x}_z + k_z\,x_z + f_m = T_{em}(v_{in} - v_h)\,, \tag{3}$$

where x_z is the actuator displacement, m_z, b_z, and k_z are the mass, damping, and stiffness, respectively, T_{em} is electromechanical transformer ratio, v_{in} is the applied (input) voltage, and v_h is the hysteresis voltage of the piezoelectric actuator model. With reference to Fig. 1, for a small displacement, an approximated linear relationship k_{zm} can be established between the piezoelectric actuator position x_z and the link A displacement x_m,

$$k_{zm} \triangleq \frac{x_z}{x_m} = \frac{l_1}{l_3}\,. \tag{4}$$

Based on the above relationships, the lumped parameter dynamic model of the piezo-driven micro/nano manipulator can be derived by substituting (2) and (4) into (3) to eliminate f_m and x_z, respectively, to yield

$$m_{lp}\,\ddot{x}_m + b_{lp}\,\dot{x}_m + k_{lp}\,x_m + v_h = v_{in}\,, \tag{5}$$

where

$$\begin{aligned} m_{lp} &= \frac{1}{T_{em}}\left(m_z\,k_{zm} + m_a + \frac{I_b + I_c}{{l_3}^2}\right)\,, \\ b_{lp} &= \frac{1}{T_{em}}\,b_z\,k_{zm}\,, \\ k_{lp} &= \frac{1}{T_{em}}\left(k_z\,k_{zm} + \frac{4\,k_{\tau_z\alpha_z}}{{l_3}^2}\right)\,. \end{aligned} \tag{6}$$

In addition to the hysteresis effect v_h described by (5), there are other nonlinear effects that are present in the flexure-based manipulator. Furthermore, there are generally external disturbances in a practical dynamical system. For these reasons, the equation of motion (5) is rewritten as

$$m_{lp}\,\ddot{x}_m + b_{lp}\,\dot{x}_m + k_{lp}\,x_m + v_n + v_d = v_{in}\,, \tag{7}$$

where v_n and v_d represent all the nonlinear effects and external disturbances, respectively, encountered in the motion system. It is understood that these terms are generally bounded, i.e. $|v_n| \leq \delta v_n$ and $|v_d| \leq \delta v_d$, where δv_n and δv_d are positive constant numbers. With the given model (7), an advanced control methodology can be established to effectively control the piezo-driven flexure-based four-bar micro/nano manipulator.

III. Sliding Mode Motion Tracking Control Methodology

For the piezo-driven flexure-based four-bar micro/nano manipulator described by (7), a sliding mode motion control methodology can be formulated for the purpose of tracking a specified motion trajectory $x_{md}(t)$. Under the proposed control approach, the physical parameters of the system are assumed to be uncertain. Furthermore, there exist bounded nonlinear effects and external disturbances within the closed-loop system. Moreover, the desired trajectory $x_{md}(t)$ is assumed to be at least twice continuously differentiable and both $\dot{x}_{md}(t)$ and $\ddot{x}_{md}(t)$ are bounded and uniformly continuous in $t \in [0, \infty)$. The established closed-loop system of (7) is required to achieve a specified goal or target performance, which is defined as

$$m_d\,\ddot{e}_p + b_d\,\dot{e}_p + k_d\,e_p = 0\,, \tag{8}$$

where m_d, b_d, and k_d are the desired constant values of mass, damping, and stiffness, respectively, and $e_p(t)$ is the position tracking error defined as $e_p(t) = x_m(t) - x_{md}(t)$.

The uncertainties of the motion system have to be modelled in the establishment of the sliding mode motion tracking control methodology. The uncertain system parameters of the manipulator (7) are modelled as

$$\begin{aligned} |\,\Delta m_{lp}\,| &= |\,m_{lp} - \hat{m}_{lp}\,| \le \delta m_{lp}\,, \\ |\,\Delta b_{lp}\,| &= |\,b_{lp} - \hat{b}_{lp}\,| \le \delta b_{lp}\,, \\ |\,\Delta k_{lp}\,| &= |\,k_{lp} - \hat{k}_{lp}\,| \le \delta k_{lp}\,, \end{aligned} \tag{9}$$

where Δm_{lp}, Δb_{lp}, and Δk_{lp} represent the parametric errors, $\hat{m}_{lp}$, $\hat{b}_{lp}$, and $\hat{k}_{lp}$ represent the estimated parameters, and the positive numbers δm_{lp}, δb_{lp}, and δk_{lp} denote the bounds of the system parameters. Furthermore, there exists an upper bound δv_{nd} of the nonlinear effects and external disturbances of (7) such that

$$|\,v_n + v_d\,| \le \delta v_n + \delta v_d \le \delta v_{nd}\,. \tag{10}$$

In the proposed model of uncertainties (9) and (10), it is assumed that the exact values of m_{lp}, b_{lp}, k_{lp}, v_n, and v_d in (7) are unknown. However, the estimated values and their corresponding bounds of the system parameters, as well as the bound of the nonlinear effects and external disturbances, are available. With this assumption, the sliding mode motion tracking control methodology can be realised.

In establishing the sliding mode motion tracking control methodology, a switching function σ is specified,

$$\sigma = \dot{e}_p + \xi\,, \tag{11}$$

where ξ is the state of a dynamic compensator used to shape the position tracking errors. The dynamic compensator can be chosen as

$$\dot{\xi} = -\,\alpha\,\xi + k_p\,e_p + k_v\,\dot{e}_p\,, \tag{12}$$

where α is a constant scalar such that $\alpha \ge 0$, and k_p and k_v are the control gains which are related to the specified target performance (8). Differentiating (11) with respect to time, yields

$$\dot{\sigma} = \ddot{e}_p + \dot{\xi}\,. \tag{13}$$

To examine the closed-loop dynamics of the system under the sliding mode motion control, the dynamic compensator (12) is substituted into (13) with the term ξ in (12) eliminated by using (11),

$$\ddot{e}_p + (k_v + \alpha)\,\dot{e}_p + k_p\,e_p = \dot{\sigma} + \alpha\,\sigma\,. \tag{14}$$

By choosing

$$\begin{aligned} k_p &= m_d^{-1}\,k_d\,, \\ k_v &= m_d^{-1}\,b_d - \alpha\,, \end{aligned} \tag{15}$$

the closed-loop dynamics (14) becomes

$$m_d\,\ddot{e}_p + b_d\,\dot{e}_p + k_d\,e_p = m_d\,(\dot{\sigma} + \alpha\,\sigma)\,. \tag{16}$$

During sliding motion where $\dot{\sigma} = 0$ and $\sigma = 0$, the closed-loop dynamics (16) achieves the target performance (8).

Theorem 1: For the piezo-driven flexure-based four-bar micro/nano manipulator described by (7) under the model of uncertainties (9) and (10), a sliding mode motion tracking control methodology is established for the manipulator to achieve the target performance (8). The control methodology is described by the following equations:

$$v_{in} = \hat{m}_{lp}\,\ddot{x}_{meq} + \hat{b}_{lp}\,\dot{x}_m + \hat{k}_{lp}\,x_m - k_s\,\sigma - d\,\frac{\sigma}{|\,\sigma\,|}\,, \tag{17}$$

where

$$\ddot{x}_{meq} = \ddot{x}_{md} - \dot{\xi}\,, \tag{18}$$

and the term d is governed by

$$d \ge \delta m_{lp}\,|\ddot{x}_{meq}| + \delta b_{lp}\,|\dot{x}_m| + \delta k_{lp}\,|x_m| + \delta v_{nd} + \epsilon\,. \tag{19}$$

The terms k_s and ϵ in (17) and (19), respectively, are any positive scalars.

Proof: For the system described by (7) with the sliding mode motion tracking control law (17), a Lyapunov function $u(\sigma)$ is proposed,

$$u(\sigma) = \frac{1}{2}\,m_{lp}\,\sigma^2\,, \tag{20}$$

which is continuous and non-negative. Differentiating $u(\sigma)$ with respect to time yields

$$\dot{u}(\sigma) = m_{lp}\,\sigma\,\dot{\sigma}\,. \tag{21}$$

From (13) and (18), the time derivative of the switching function is given by

$$\dot{\sigma} = \ddot{x}_m - \ddot{x}_{meq}\,, \tag{22}$$

and (21) is rewritten as

$$\begin{aligned} \dot{u}(\sigma) &= \sigma\,(m_{lp}\,\ddot{x}_m - m_{lp}\,\ddot{x}_{meq})\,, \\ &= \sigma\,(v_{in} - b_{lp}\,\dot{x}_m - k_{lp}\,x_m - v_n \\ &\quad -v_d - m_{lp}\,\ddot{x}_{meq})\,, \end{aligned} \tag{23}$$

where the term $(m_{lp}\,\ddot{x}_m)$ is modified by using (7). Substituting the control law (17) into (23) to replace the term v_{in} and using the model of uncertainties (9) and (10),

$$\begin{aligned}\dot{u}(\sigma) &= -k_s\,\sigma^2 - d\,|\,\sigma\,| + \sigma\,[\,-\Delta m_{lp}\,\ddot{x}_{meq} - \Delta b_{lp}\,\dot{x}_m \\ &\quad - \Delta k_{lp}\,x_m - v_n - v_d\,]\,, \\ &\leq -k_s\,\sigma^2 - d\,|\,\sigma\,| + |\,\sigma\,|\,[\,|\,\Delta m_{lp}\,\ddot{x}_{meq}\,| \\ &\quad + |\,\Delta b_{lp}\,\dot{x}_m\,| + |\,\Delta k_{lp}\,x_m\,| + |\,v_n + v_d\,|\,]\,, \\ &\leq -k_s\,\sigma^2 - d\,|\,\sigma\,| + |\,\sigma\,|\,[\,\delta m_{lp}\,|\,\ddot{x}_{meq}\,| \\ &\quad + \delta b_{lp}\,|\,\dot{x}_m\,| + \delta k_{lp}\,|\,x_m\,| + \delta v_{nd}\,]\,. \end{aligned} \tag{24}$$

Replacing the term d in (24) by using (19) yields

$$\dot{u}(\sigma) \leq -k_s\,\sigma^2 - \epsilon\,|\,\sigma\,|\,. \tag{25}$$

This shows that $u(\sigma) \to 0$ (which in turn implies that $\sigma \to 0$) as $t \to \infty$. Both the stability of the closed-loop system and the convergence of the motion tracking are guaranteed by the proposed sliding mode motion control law (17) driving the system (7) to reach the target performance (8). ■

In the implementation of the control law (17), the discontinuous function $\frac{\sigma}{|\sigma|}$ will give rise to control chattering due to imperfect switching in the computer control. This is undesirable, as un-modelled high frequency dynamics might be excited. To eliminate this effect, the concept of boundary layer technique [18] is applied to smooth the control signal. In a small neighbourhood of the sliding surface ($\sigma = 0$), the discontinuous function is replaced by a saturation function, which is defined as

$$\text{sat}(\frac{\sigma}{\Delta}) = \begin{cases} -1 & : \quad \sigma < -\Delta\,, \\ \sigma/\Delta & : \quad -\Delta \leq \sigma \leq \Delta\,, \\ +1 & : \quad \sigma > \Delta\,, \end{cases} \tag{26}$$

where Δ is the boundary layer thickness, and the control law (17) becomes

$$v_{in} = \hat{m}_{lp}\,\ddot{x}_{meq} + \hat{b}_{lp}\,\dot{x}_m + \hat{k}_{lp}\,x_m - k_s\,\sigma - d\,\text{sat}(\frac{\sigma}{\Delta})\,. \tag{27}$$

With the introduction of the saturation function (26) in the control law (27), the accuracy of the switching function σ is guaranteed to stay within the boundary layer. From the closed-loop dynamics (16) of the control law, the steady-state switching function σ_{ss} within the boundary layer is obtained as

$$\sigma_{ss} = \frac{k_d\,e_{pss}}{m_d\,\alpha}\,, \tag{28}$$

where e_{pss} is the steady-state position error. As (28) describes the relationship between the steady-state position error and the steady-state switching function, it can therefore be used to select the boundary layer thickness Δ in the control implementation.

The selection of the target performance for the control system is straightforward. This is performed by comparing (8) to a standard second-order characteristic equation,

$$s^2 + 2\,\zeta\,w_n\,s + w_n^2 = 0\,, \tag{29}$$

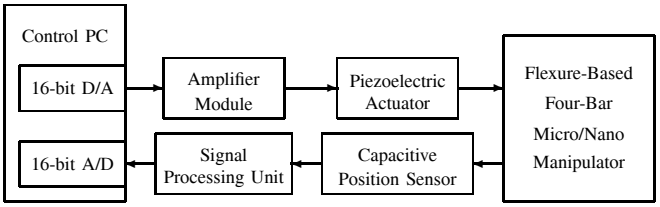

Fig. 3. Block diagram of the experimental architecture

where s, ζ, and w_n are the Laplace operator, damping ratio, and undamped natural frequency, respectively, the desired parameters are obtained as

$$m_d = 1\,, \quad b_d = 2\,\zeta\,w_n\,, \quad \text{and} \quad k_d = w_n^2\,. \tag{30}$$

As the desired response is selected through ζ and w_n, the control gains k_p and k_v in (15) can therefore be calculated from (30).

IV. Experimental Study

In order to investigate the proposed sliding mode motion tracking control methodology for the piezo-driven flexure-based four-bar micro/nano manipulator, an experimental research facility has been established. The architecture of the experimental set-up is detailed in the block diagram as shown in Fig. 3. It consists of a flexure-based four-bar mechanism, a piezoelectric actuator, an amplifier module, a capacitive position sensor, a signal processing unit, and a control PC comprising a digital-to-analogue (D/A) board and an analog-to-digital (A/D) board.

The flexure-based four-bar mechanism is established based on a flexure-hinged structure, and the piezoelectric actuator is acquired from Physik Instrumente (PI) [19]. This piezoelectric actuator is a multi-layer PZT stacked ceramic translator capable of displacement of up to 45 (μm) corresponding to a range of operating voltage from 0 to 100 (V). The PI amplifier module has a fixed output gain of 10 providing a voltage range from -20 to $+120$ (V), and the PI capacitive position sensor has a measurement range of up to 50 (μm). The signal processing unit is used to process the position signal and is connected between the capacitive sensor and control PC. A standard desktop computer is used as the control PC. It is equipped with a Pentium 4 3.2 (GHz) processor running on an operating system capable of hard real-time control. The D/A and A/D boards within the control PC are of 16-bit resolution, and they are used to generate the control signal and to acquire the position of the micro/nano manipulator, respectively. In the experiments, the sampling frequency of the control loop is set at 2.5 (kHz).

Under the proposed control methodology, the closed-loop system is required to follow a 'jerk-free' desired motion trajectory, which is shown in Fig. 4 for position, velocity, and acceleration. The purpose is to eliminate the possibility of exciting the structural resonance of the flexure-based mechanism. This desired motion trajectory is formed by segments of higher-order 4-5-6-7 polynomials [20] with zero acceleration at the beginning and the end.

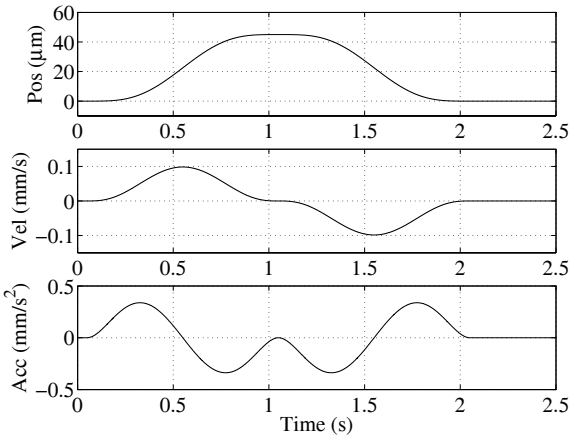

Fig. 4. 'Jerk-free' desired motion trajectory

TABLE I
LUMPED PARAMETERS OF THE PIEZO-DRIVEN FLEXURE-BASED FOUR-BAR MICRO/NANO MANIPULATOR

Lumped Parameter	Estimated Value	Bound
Mass (Vs^2/m) :	$\hat{m}_{lp} = 1$	$\delta m_{lp} = 1$
Damping (Vs/m) :	$\hat{b}_{lp} = 1 \times 10^3$	$\delta b_{lp} = 1 \times 10^3$
Stiffness (V/m) :	$\hat{k}_{lp} = 1 \times 10^6$	$\delta k_{lp} = 1 \times 10^6$
Non-Linearities and External Disturbances (V) :		$\delta v_{nd} = 30$

In this experimental study, the experiments serve not only to validate the theoretical formulation of the control methodology but also to examine the effectiveness of the proposed approach in a physical system. For the piezo-driven flexure-based four-bar micro/nano manipulator described by (7), the sliding mode motion tracking control law (27) is implemented in the control PC. With the desired motion trajectory, as shown in Fig. 4, the tracking ability of the control system can be closely evaluated experimentally in the presence of parametric uncertainties, non-linearities, and external disturbances.

Table I summarises the lumped parameter values of the manipulator for the experiments. The other control parameters are selected as follows.

A critically damped response, $\zeta = 1.0$, and an undamped natural frequency of $w_n = 157.08\ (rad/s)$ are chosen. The desired parameters in (30) are calculated as $m_d = 1\ (Vs^2/m)$, $b_d = 314\ (Vs/m)$, and $k_d = 24,674\ (V/m)$. The constant scalar α in (12) is set as $\alpha = 1\,(1/s)$ and the control gains k_p and k_v in (15) are calculated from (30) as $k_p = 24,674\ (1/s^2)$, and $k_v = 313\ (1/s)$. The steady-state position error in (28) is specified as $e_{pss} \leq 0.1\,(\mu m)$, and the steady-state value σ_{ss} is calculated as $\sigma_{ss} \leq 2.5\,(mm/s)$. The boundary layer thickness Δ in (26) is therefore chosen as the maximum value of σ_{ss}, i.e. $\Delta = 2.5\ (mm/s)$. The positive scalar ϵ in (19) is specified as $\epsilon = 1\,(V)$ and k_s of the control law (27) is adjusted to $k_s = 100\,(Vs/m)$.

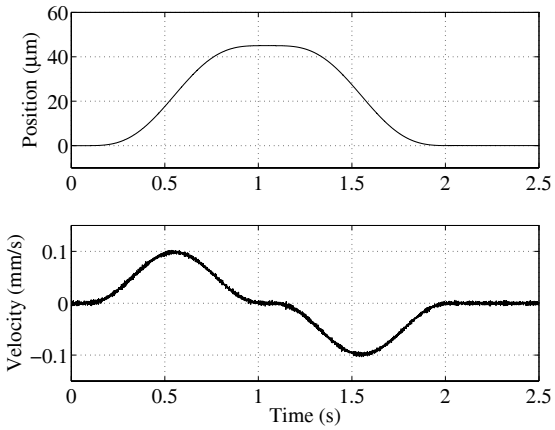

Fig. 5. Actual positions and estimated velocities

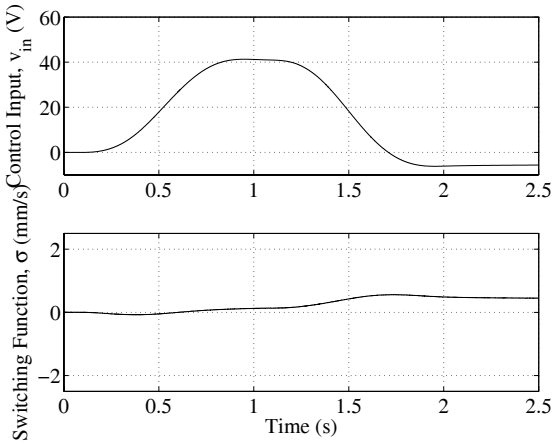

Fig. 6. Control input and switching function

V. RESULTS AND DISCUSSION

Tracking the given desired motion trajectory as shown in Fig. 4, the resulting positions and estimated velocities of the manipulator are shown in Fig. 5. Despite parametric uncertainties, nonlinear effects, and external disturbances in the motion system, the proposed sliding mode motion tracking control law (27) showed a precise tracking ability.

The control input v_{in} and switching function σ are shown in Fig. 6. The switching function indicates that the proposed closed-loop system operated well within the specified boundary layer thickness Δ. This implies that the closed-loop system tracked the desired motion trajectory closely with the switching function kept to a minimum. The position and velocity tracking errors are shown in Fig. 7. These results show that the position and velocity tracking errors were confined within $0.07\ (\mu m)$ and $0.008\ (mm/s)$, respectively, during dynamic motion. Furthermore, the position tracking errors were less than $0.03\ (\mu m)$ at steady-state. These steady-state results were almost at the noise level of the closed-loop system. On the whole, the resulting tracking errors indicate that the control law had successfully accommodated the aforementioned conditions in the closed-loop system. In addition, the effectiveness of the proposed

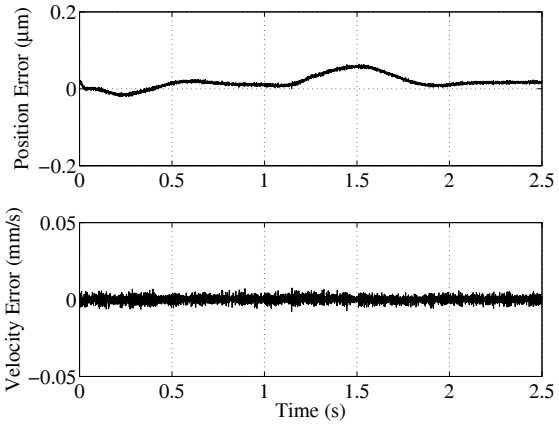

Fig. 7. Position and velocity tracking errors

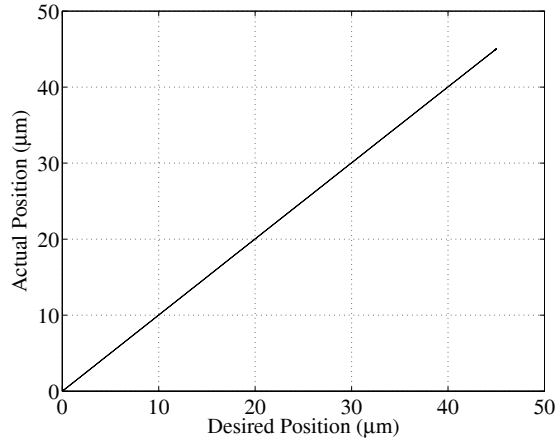

Fig. 8. Actual displacement against desired positions

control methodology was demonstrated as shown in the plot of the actual displacement against desired positions in Fig. 8. Moreover, it must be noted that the control experiments were conducted numerous times and the results were repeatable experimentally.

The proposed sliding mode motion tracking control methodology is shown to be stable, robust, and capable of tracking the desired motion trajectory under uncertain system parameters, non-linearities, and external disturbances.

VI. Conclusions

A motion tracking control methodology based on sliding mode strategy has been proposed and investigated for the tracking of desired motion trajectories in the flexure-based micro/nano manipulator driven by a piezoelectric actuator. The proposed control methodology is formulated to accommodate uncertain system parameters, non-linearities including the hysteresis effect, and external disturbances in the micro/nano manipulation system.

Stability of the closed-loop system has been analysed and the convergence of the position tracking errors to zero is guaranteed by the proposed control methodology. Furthermore, a high-precision tracking performance has also been demonstrated in the experimental study.

Acknowledgment

This work is supported by an Australian Research Council (ARC) Linkage Infrastructure, Equipment and Facilities (LIEF) grant and an ARC Discovery grant.

References

[1] K. Spanner and S. Vorndran, "Advances in piezo-nanopositioning technology," in *Proceedings of 2003 IEEE/ASME International Conference on Advanced Intelligent Mechatronics*, vol. 2, Kobe, Japan, 20–24 July 2003, pp. 1338–1343.

[2] P. Gao, S.-M. Swei, and Z. Yuan, "A new piezodriven precision micropositioning stage utilizing flexure hinges," *Nanotechnology*, vol. 10, no. 4, pp. 394–398, December 1999.

[3] S. H. Chang, C. K. Tseng, and H. C. Chien, "An ultra-precision XYθ_z piezo-micropositioner. I. Design and analysis," *IEEE Transactions on Ultrasonics, Ferroelectrics, and Frequency Control*, vol. 46, no. 4, pp. 897–905, July 1999.

[4] T.-F. Lu, D. C. Handley, Y. K. Yong, and C. Eales, "A three-DOF compliant micromotion stage with flexure hinges," *Industrial Robot*, vol. 31, no. 4, pp. 355–361, 2004.

[5] G. Alici and B. Shirinzadeh, "Kinematics and stiffness analyses of a flexure-jointed planar micromanipulation system for a decoupled compliant motion," in *Proceedings of 2003 IEEE/RSJ International Conference on Intelligent Robots and Systems*, vol. 3, Las Vegas, Nevada, 27–31 October 2003, pp. 3282–3287.

[6] M. Goldfarb and N. Celanovic, "Modeling piezoelectric stack actuators for control of micromanipulation," *IEEE Control Systems Magazine*, vol. 17, no. 3, pp. 69–79, June 1997.

[7] H. J. M. T. A. Adriaens, W. L. de Koning, and R. Banning, "Modeling piezoelectric actuators," *IEEE/ASME Transactions on Mechatronics*, vol. 5, no. 4, pp. 331–341, December 2000.

[8] Y. I. Somov, "Modelling physical hysteresis and control of a fine piezodrive," in *Proceedings of 2003 International Conference Physics and Control*, vol. 4, St. Petersburg, Russia, 20–22 August 2003, pp. 1189–1194.

[9] J.-J. Tzen, S.-L. Jeng, and W.-H. Chieng, "Modeling of piezoelectric actuator for compensation and controller design," *Precision Engineering*, vol. 27, no. 1, pp. 70–86, January 2003.

[10] X. Dang and Y. Tan, "An inner product-based dynamic neural network hysteresis model for piezoceramic actuators," *Sensors and Actuators, A: Physical*, vol. 121, no. 2, pp. 535–542, 30 June 2005.

[11] T. Chang and X. Sun, "Analysis and control of monolithic piezoelectric nano-actuator," *IEEE Transactions on Control Systems Technology*, vol. 9, no. 1, pp. 69–75, January 2001.

[12] H.-J. Shieh, F.-J. Lin, P.-K. Huang, and L.-T. Teng, "Adaptive tracking control solely using displacement feedback for a piezo-positioning mechanism," *IEE Proceedings of Control Theory and Applications*, vol. 151, no. 5, pp. 653–660, 23 September 2004.

[13] G. Song, J. Zhao, X. Zhou, and J. A. D. Abreu-García, "Tracking control of a piezoceramic actuator with hysteresis compensation using inverse Preisach model," *IEEE/ASME Transactions on Mechatronics*, vol. 10, no. 2, pp. 198–209, April 2005.

[14] H. C. Liaw, D. Oetomo, G. Alici, and B. Shirinzadeh, "Special class of positive definite functions for formulating adaptive micro/nano manipulator control," in *Proceedings of 9th IEEE International Workshop on Advanced Motion Control*, Istanbul, Turkey, 27–29 March 2006, pp. 517–522.

[15] H. C. Liaw, D. Oetomo, B. Shirinzadeh, and G. Alici, "Robust motion tracking control of piezoelectric actuation systems," in *Proceedings of 2006 IEEE International Conference on Robotics and Automation*, Orlando, Florida, 15–19 May 2006, pp. 1414–1419.

[16] S. T. Smith, *Flexure: elements of elastic mechanisms*. Boca Raton, Florida: CRC Press, 2000.

[17] J. M. Paros and L. Weisbord, "How to design flexure hinges," *Machine Design*, vol. 37, no. 27, pp. 151–156, 25 November 1965.

[18] J.-J. E. Slotine and W. Li, *Applied nonlinear control*. Englewood Cliffs, New Jersey: Prentice-Hall, 1991.

[19] S. Vorndran, Ed., *PI catalog: the world of micro- and nanopositioning 2005/2006*. Karlsruhe, Germany: The PI-Polytec Group, 2005.

[20] J. Angeles, *Fundamentals of robotic mechanical systems: theory, methods, and algorithms*. New York: Springer, 2003.